Eur. Phys. J. D **38**, 553–562 (2006)
DOI: 10.1140/epjd/e2006-00060-0

THE EUROPEAN PHYSICAL JOURNAL D

Quantum entanglement in an oscillating macroscopic mirror

J.W. Eslick Jr, H.N. Pham, C. Radu, and A. Puri[a]

Department of Physics, University of New Orleans, New Orleans, Louisiana 70148, USA

Received 12 June 2005 / Received in final form 28 October 2005
Published online 28 March 2006 –

Abstract. In this paper, we revisit the problem of quantum entanglement in an oscillating macroscopic mirror previously studied by Marshall et al. consisting of a modified Michelson interferometer where one of the mirrors is free to oscillate about its center of mass. A photon incident upon the oscillating mirror becomes entangled with the mirror, driving the mirror into a superposition of quantum states. Once the photon and mirror decouple, the mirror returns to its initial state. The purpose of our investigations was to optimize the parameter regime, taking into consideration the current state of technology and the demands imposed by the need to maintain a stable environment in the presence of thermal noise. Optimization should not demand ultra-low temperatures and this is reflected in our results. Our results also show that if the separation between states is maintained at 10^{-14} m, the mirror size is reduced, making it easier to induce superposition in the mirror. The critical nature of mirror reflectivity and its connection to cavity decay rate was also revealed by our investigations. The results obtained through our investigations could be useful in quantum error correction, where decoherence negatively affects the results of computations performed by quantum computers. Finally, we note that we are only concerned with an isolated system, where no losses to the external environment occur and any decoherence that occurs within the system remains internal to the system; that is, any mention of decoherence refers specifically to recoverable decoherence.

PACS. 03.65.-w Quantum mechanics – 07.05.Kf Data analysis: algorithms and implementation; data management – 42.25.Hz Interference – 42.25.Kb Coherence

1 Introduction

Schrödinger's famous thought experiment which led to the conclusion that a cat can exist in a superposition of states, a state of being alive and a state of being dead, showed that even macroscopic systems would, in theory, exhibit quantum mechanical properties. Environmental conditions lead to decoherence and a subsequent loss of certainty. This has been a constant problem for investigation of macroscopic systems exhibiting a superposition of states.

Marshall et al. [1] describes a Schrödinger cat experiment in which the cat is replaced by a mirror. This experiment proposes a modified Michelson interferometer as shown in Figure 1b. A single photon is emitted from a source and passes through a beam splitter followed by a semi-reflecting mirror initially oscillating about its center of mass with a pre-determined frequency. The amplitude of the mirror's oscillation should be large enough to overcome any inherent uncertainty in the position of the center of mass of the mirror due to random quantum fluctuations of its atoms. Thus, a change in the mirror's position could more easily be detected.

The photon has two equally probable destinations: a fixed mirror at the end of cavity A or a micro-mechanical oscillator at the end of cavity B. If the photon interacts with the mirror in cavity B, then its motion is altered by the radiation pressure of the photon. Due to the non-deterministic nature of quantum mechanics, however, one can not say with absolute certainty which path the photon will "choose" to take. Only the probability that a given path will be taken can be determined. Moreover, due to the oscillation of the micro-mirror, there is a nonzero path difference between the cavities creating self-interference of the photon [2]. The photon will interact with the oscillating mirror for one full period of the mirror's motion; however, the "amount" of photon remaining in the cavities will decay over this period due to transmission losses by the mirror and random thermal fluctuations of its atoms.

However, at the end of a period, what remains of the photon will leak out of the cavity where it is detected at detector 1 or detector 2, creating an interference "pattern" for the mirror. Thus, interference visibility for the photon-mirror system will provide a measure of the amount of decoherence in the system over the period of motion of the oscillating mirror. Furthermore, this interference visibility will be increased for a mirror with sufficiently large amplitude of oscillation.

[a] e-mail: apuri@uno.edu

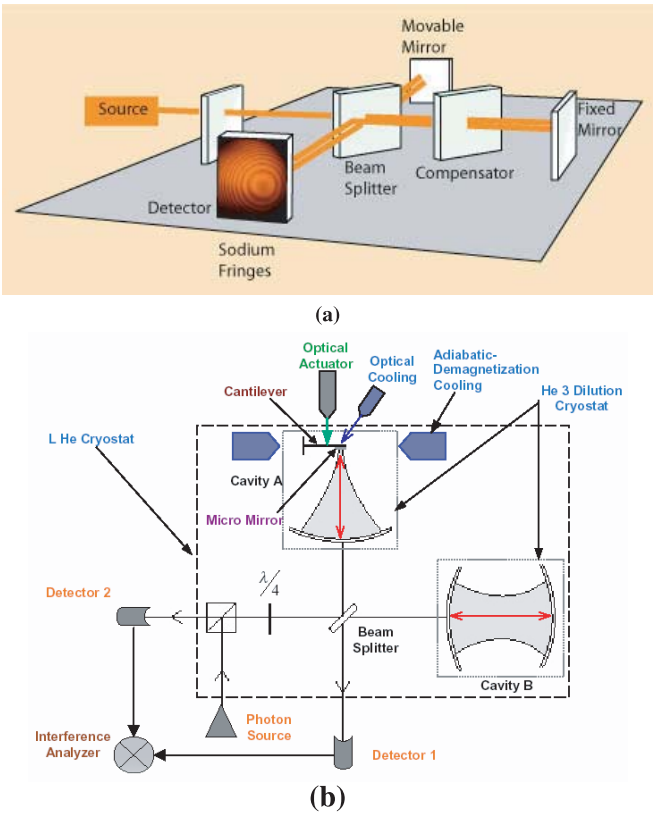

Fig. 1. (a) The Michelson interferometer produces interference fringes by splitting a beam of photons so that one beam strikes a fixed mirror and the other one a movable mirror. When the reflected beams are brought back together, interference pattern results. From the interference pattern we can characterize the position of the moving mirror. This method is one of the most sensitive methods for measuring the displacement of objects, being used also to detect gravitational waves and for high precision positioning. In the figure, one path comprises three crossings of the beam splitter while another only one crossing. To re-establish equality of optical paths in the glass, a $\lambda/4$ compensating plate is inserted. (b) Set-up as used in [1] modified to induce ultra-low temperatures in the oscillating mirror's environment.

1.1 Environmental conditions

Due to the extreme sensitivity of the components involved, environmental conditions must be carefully controlled. The mirror cannot be allowed to interact with air molecules, so ultra-high vacuum conditions are necessary. In addition, thermal fluctuations of the mirror's atoms will affect the path of its motion and increase the decoherence rate. Thus, temperature is of primary consideration. Temperatures on the order of 60 μK are necessary for optimal results at low mirror frequencies. Extremely high quality mirrors are also necessary to minimize transmission losses [3].

In order to ensure the return of the oscillating mirror to its ground state, the values of the feedback laser's gain factor g and the cavity decay rate γ_c must be considered simultaneously. If a small gain factor is required, then a correspondingly high value of γ_c is necessary. Conversely, if a small value of γ_c is required, then a correspondingly high value of g is necessary.

Experimental parameter regimes that satisfy the physical constraints based on a particular experimental geometry have been examined by Bose et al. [4] It was determined that for a 1 cm cavity, γ_c must be at least 10^6 s^{-1} for moving mirrors [at least 10 s^{-1} for stationary mirrors] and for a 10 μm cavity, γ_c must be at least 10^7 s^{-1}. Furthermore, they show that in order for decoherence not to occur too rapidly, the mirror frequency must be about the same as the decoherence rate.

This paper addresses the question of how to further reduce the sources of quantum decoherence. This is achieved by optimizing the parameters subject to all physical and geometrical constraints of the problem and thus an optimum viable experimental configuration is proposed.

1.2 Optimization of parameters

We propose an optimization of the parameters involved which would allow the experiment to be performed utilizing current technology, reduce decoherence by minimizing photon leakage from the cavity by increasing the quality factor of the oscillator, return the mirror closer to its ground state, satisfy the constraints, and work with an environmental temperature that is easier to achieve. The first, third, and fourth objectives can be realized by finding parameter values that simultaneously minimize the energy of the cooled mirror and satisfy the constraints imposed on the set-up. The second objective can be accomplished by improving the quality of the optical cavities and replacing the mechanical oscillator with an optical actuator. The third objective can be accomplished by choosing a sufficiently high frequency for the oscillating mirror. The optimization of parameters that we propose in this paper are important to the realization of the experiment. As originally proposed, the constraints could not all be satisfied. In particular, the cavity's decay rate in [1] is much higher than would be required by the constraints. However, cavities can not as yet be constructed with decay rates as low as would be necessary. Thus, our work helps to ensure that this experiment can indeed be performed.

The plan of the paper is as follows: in Section 2, we outline the basic experimental set-up. Based on environmental considerations, we present an improved set-up which can detect interference visibility at very low temperatures. Section 3 is devoted to a brief review of the mathematical formulation of the problem [1]. Experimental constraints are presented in Section 4. Numerical results are presented in Section 5. Finally, Section 6 is devoted to a brief discussion of our results.

1.3 Motivation

Our investigations have been motivated by the need for reliable error correction methods in Quantum Computing. In 1982, Feynman gave the first formal description of a machine capable of using the principles of quantum mechanics to simulate physical processes [5]. His idea has

Table 1. The parameters used by the authors of [1].

$\omega_m/2\pi$ (Hz)	γ_m (s^{-1})	P (W)	γ_c (s^{-1})	M (kg)	η	L (m)	g	T_E (K)
500	0.03	10^{-8}	3×10^7	5×10^{-12}	0.8	0.05	6×10^5	2×10^{-3}

led to the modern concept of a quantum computer. A quantum computer is a device in which computations are carried out by placing one or more units of qubits into a superposition of two states; where, a qubit is an information "particle". One state is equivalent to a boolean state 0 and the second to a boolean state 1. Thus, there is a probability of the qubit being in state 0 as well as a probability of the qubit being in state 1; where, for a qubit in superposition, both probabilities are simultaneously nonzero. A quantum computer would execute commands by operating on sequences of qubits, thereby producing new states.

Unfortunately, constructing a quantum computer of the size needed to solve formidable problems turns out to be a difficult problem. Environmentally induced decoherence destroys the superposition states introducing errors into the computations [6]. A coherent state must be maintained for small couplings and for very short time intervals [7]. Thus, the problem of decoherence is a hurdle that must be cleared before any real gains in quantum computing can be made.

Although (environmentally induced) decoherence has been an ongoing problem in quantum computing, there have been recent advances. Research has been conducted in the area of quantum error correction [8]. Here, a system in which the amount of decoherence can be measured and minimized is used to fine-tune the quantum system as needed. Thus, it acts as a sort of gauge to adjust the parameters of the quantum system to minimize errors.

The apparatus described in our paper would be quite useful in this capacity. With an optimal parameter regime defined, it would provide a system capable of inducing superposition in a bacterium-sized object that would remain in this superposed state long enough to provide information that could be applied to error correction of quantum systems. The error correction apparatus would be isolated from the external environment thereby reducing environmentally induced decoherence. Furthermore, at high frequencies, it could be maintained at near room temperature making it easier to implement and control.

2 Experimental considerations

The temperature of the oscillating mirror's environment is one of the most important factors in determining how the experiment is set-up and conducted. Not only does it control how the set-up is designed, but also has a great effect on decoherence rate and interference visibility.

However, our analysis revealed the fact that the temperature itself is affected by the mirror's frequency. Thus, there are two parameter regimes of interest: one with a low oscillator frequency and another with a high oscillator frequency.

2.1 High frequency regime

For high frequencies, it is not necessary to maintain the ultra-low temperatures required by the lower frequencies. For example, for a frequency of 10 MHz, a temperature of ∼302 K is all that is required! Figure 1 illustrates a set-up that will suffice for this regime (see also Tab. 1). This set-up uses a modified Michaelson interferometer. In it, two equal length optical cavities are used to transport a single photon. At the end of each cavity is a mirror. One cavity contains a large, rigid mirror while the other contains a micro-mirror attached to a mechanical oscillator. The frequency of the oscillator, hence of the mirror, creates a path difference between the two cavities. It is this path difference that puts the photon into superposition, which is transferred to the mirror during their entanglement. While lower temperatures help maintain a stable environment, no adaptations must be made to the set-up when working with higher temperatures.

2.2 Low frequency regime

For low frequencies, a colder environment is needed, perhaps as low as 60 μK. We were able to achieve an optimized set of parameters for a frequency of ∼300 Hz with an environmental temperature of ∼2.7 mK (somewhat higher than the temperature used in [1]). At this frequency and temperature, effects on the decoherence rate and interference visibility became quite apparent. Lower temperatures would be desirable; in fact, they would be necessary for even lower frequencies. Figure 1b illustrates an experimental set-up designed to achieve an ultra-cool environment.

Detectors 1 and 2 are avalanche photon detectors, capable of detecting a single photon. The photon source is a single photon emission laser that provides a short burst of photons. Cavities A and B are Fabry-Pérot cavities specific to a Michaelson interferometer, which can provide good detection in the case of a weak perturbation. The cantilever is a Si cantilever with high Q ($\sim 10^6$) that can be put in oscillation by a weak excitation [9]. The optical actuator uses the radiation pressure of the photon to make the cantilever oscillate giving a very low inertia to the oscillation, which is very stable in frequency [10]. The micro-mirror is a high reflectivity (SiO_2/TiO_2) multilayer structure. The cooling process has four stages: liquid He (1.8 K), He_3 dilution (2 mK), optical cooling [11] and/or adiabatic-demagnetization cooling (60 mK).

3 Mathematical formulation

In this section, we present, for completeness, a brief review of the mathematical formulation of the problem [1].

The Hamiltonian for the photon-mirror system is given by

$$H = \hbar\omega_c a^\dagger a + \hbar\omega_m b^\dagger b - \hbar G a^\dagger a(b + b^\dagger) \tag{1}$$

where $a^\dagger$ and a are the creation and annihilation operators for the photon in the cavity and ω_c is its (angular) frequency, $b^\dagger$ and b are the creation and annihilation operators for the phonon generated by the center-of-mass motion of the mirror, ω_m is the mirror's (angular) frequency, and $G = (\omega_c/L)\sqrt{\hbar/2M\omega_m}$ is the coupling constant of the photon/mirror system, with M being the mass of the oscillating mirror [12].

Let $|\alpha\rangle$ and $|\beta\rangle$ denote the initial state of the photon and mirror respectively. Suppose that the photon is initially in a superposition of states of being in cavity A and cavity B and the mirror is initially in a coherent state. Then the state of the photon and the mirror after a time t are [12]

$$|\alpha(t)\rangle = \frac{1}{\sqrt{2}}\left(|1\rangle_{\mathrm{A}}|0\rangle_{\mathrm{B}} + |0\rangle_{\mathrm{A}}|1\rangle_{\mathrm{B}}\right)e^{-i\omega_c t} \tag{2}$$

and

$$|\beta(t)\rangle = \left[e^{-\frac{|\beta|^2}{2}}\sum_{n=0}^{\infty}\frac{\beta^n}{\sqrt{n!}}|n\rangle\right]e^{-i\omega_m t} \tag{3}$$

respectively, with $|n\rangle$ being the nth eigenstate of an harmonic oscillator.

For the entangled system, however, the mirror motion is perturbed by the photon's momentum due to the radiation pressure it exerts on the mirror [13]. Putting $\kappa = G/\omega_m$ as the quantity used to measure the displacement of the mirror's center of mass in units of coherent state wavepacket lengths, we obtain the state of the entangled mirror/photon system after a time t [12]

$$\begin{aligned}|\psi(t)\rangle = \frac{1}{\sqrt{2}}e^{-i\omega_c t}\Big(&e^{i\kappa^2(\omega_m t - \sin\omega_m t)}|1\rangle_{\mathrm{A}}|0\rangle_{\mathrm{B}} \\ &\times\left|\beta e^{-i\omega_m t} + \kappa\left(1 - e^{-i\omega_m t}\right)\right\rangle\Big) \\ &+ \frac{1}{\sqrt{2}}e^{-i\omega_c t}|0\rangle_{\mathrm{A}}|1\rangle_{\mathrm{B}}\left|\beta e^{-i\omega_m t}\right\rangle\end{aligned} \tag{4}$$

and the initial state of the system is

$$|\psi(0)\rangle = \frac{1}{\sqrt{2}}(|1\rangle_{\mathrm{A}}|0\rangle_{\mathrm{B}} + |0\rangle_{\mathrm{A}}|1\rangle_{\mathrm{B}})|\beta\rangle. \tag{5}$$

The off-diagonal element of the photon's reduced energy matrix as obtained in [1] is

$$\frac{1}{2}e^{-\kappa^2(1-\cos\omega_m t)}e^{i\kappa^2(\omega_m t - \sin\omega_m t) + i\kappa\mathrm{Im}\left[\beta\left(1-e^{i\omega_m t}\right)\right]}. \tag{6}$$

By averaging equation (6) over β using a Gaussian probability distribution defined by [12] $(1/\pi\bar{n})e^{-|\beta|^2/\bar{n}}$, where $\bar{n} = \left(e^{\hbar\omega_m/k_B T_E} - 1\right)^{-1}$ is the mean number of thermal excitations of a mirror in a thermal state and T_E is the environmental temperature, one can obtain the maximum time-dependent interference visibility V for a mirror in a thermal state as

$$V = e^{-\kappa^2(2\bar{n}+1)(1-\cos\omega_m t)}. \tag{7}$$

The time-dependent decoherence rate is defined as [4]

$$\gamma_D(t) = \frac{4k^2\gamma_m k_B T_E}{\hbar\omega_m}(1 - \cos\omega_m t)^2, \tag{8}$$

where k is a quantum number. Here, k is taken to be one, so

$$\gamma_D(t) = \frac{4\gamma_m k_B T_E}{\hbar\omega_m}(1 - \cos\omega_m t)^2. \tag{9}$$

Therefore, the average decoherence rate over one period of the mirror's motion is

$$\overline{\gamma_D} = \frac{\gamma_m k_B T_E M(\Delta x)^2}{\hbar^2}, \tag{10}$$

where the spatial separation between quantum states, Δx, is required to be much larger than the width of an individual wave packet [12]. Furthermore, if $\kappa^2 \geq 1$ (see *Constraints* below), then the spatial displacement of the mirror will be larger than the uncertainty in the position of its center of mass due to random thermal fluctuations of its atoms; thereby producing distinct positions of the mirror. Thus, $\Delta x \sim \sqrt{\hbar/M\omega_m}$, and

$$\overline{\gamma_D} \sim \frac{\gamma_m k_B T_E}{\hbar\omega_m}. \tag{11}$$

Finally, the final energy of the cooled mirror is given by [13]

$$E_c = \frac{\hbar\omega_m}{2}\frac{1}{2(1+g)}\left[\frac{4k_B T_E}{\hbar\omega_m} + 2\xi + \frac{g^2}{\eta\xi}\right], \tag{12}$$

where g is the gain factor of the cooling laser, η is the detection efficiency, and ξ is defined by

$$\xi = \frac{64\pi cP}{M\gamma_m\omega_m\lambda\gamma_c^2 L^2}, \tag{13}$$

with P being the intensity of the source light (incident on the measurement cavity), M the mass of the oscillating mirror, γ_m the damping rate of the mirror's motion, and γ_c the cavity decay rate. The first term in equation (12) arises due to thermal noise in the system. The second term in equation (12) is due to both the back action noise from the source light as well as the back action noise from the feedback laser. The third term in equation (12) is due to the noise associated with imprecision in measurement. We note that equation (12) has been modeled on equation (58) in [13]; but, due to the large feedback gain required, a second laser must be used to supply the necessary feedback force used to cool the mirror down to its ground state.

The feedback force supplied by this additional laser must have a constant component that balances the back action from the measurement field. As needed, the feedback laser supplies an additional "kick" to the mirror to dampen its motion allowing the mirror to settle into a steady state. Once the mirror is cooled to its ground state and is no longer oscillating, both the source light and the feedback laser are simultaneously switched off, trapping a photon in the cavity. Interference can then be measured and the process is repeated. However, the addition of this second laser contributes noise to the system that must be accounted for in equation (12).

4 Constraints

Two types of constraints must be considered in the determination of a set of parameters for the problem. Some constraints arise due to the physical nature of the problem. Others arise due to limitations on measurement or technology.

4.1 Constraint #1

For the superposition to involve two distinct mirror locations, the spatial separation Δx between superposed peaks must be at least of the same order as the width of a single peak. This will ensure that the components of the Schrödinger's cat will be sufficiently separated in space, by at least as much as the spatial width of each of the cat's components. We know that the width of each of the components of the cat is equal to the width of a coherent state. Thus $\kappa^2 \gtrsim 1$.

Moreover, if N is the number of round trips made by the photon in the cavity during one period of the mirror's motion, L the cavity's length, and c the speed of light, then

$$\frac{2NL}{c} = \frac{2\pi}{\omega_m}. \tag{14}$$

Equation (2) can then be used with equation (14) to get

$$\kappa^2 = \frac{\hbar N^3 L \omega_c^2}{2\pi^3 c^3 M}. \tag{15}$$

Thus, the condition $\kappa^2 \gtrsim 1$ implies

$$\frac{2\hbar N^3 L}{\pi c M \lambda^2} \gtrsim 1. \tag{16}$$

4.2 Constraint #2

To ensure the separation of superposition states Δx is not due solely to random thermal fluctuations, Δx must be larger than the initial uncertainty in the mirror's position. That is, Δx must be larger than the deBroglie wavelength $\lambda_{th} = \hbar/\sqrt{2Mk_BT_E}$,

$$\Delta x > \frac{\hbar}{\sqrt{2Mk_BT_E}}. \tag{17}$$

4.3 Constraint #3

To facilitate the measurement of coherent states, the decay rate should not be larger than one period of the mirror's motion; that is, $\overline{\gamma_D} \lesssim \omega_m$. Thus,

$$\frac{\gamma_m k_B T_E}{\hbar \omega_m} \lesssim \omega_m, \tag{18}$$

or

$$\frac{k_B T_E}{\hbar \omega_m} \lesssim \frac{\omega_m}{\gamma_m} = Q, \tag{19}$$

where Q is the quality factor of the mechanical oscillator.

4.4 Constraint #4

The photon and mirror must remain coupled throughout the entire period of the mirror's motion. Thus, $\gamma_c \lesssim \omega_m$. In fact, we require $\gamma_c \lesssim \overline{\gamma_D}$, since for decoherence to remain in the system, the photon must still be present in the cavity. Thus, we have from constraint #3,

$$\gamma_c \lesssim \overline{\gamma_D} \lesssim \omega_m.$$

4.5 Constraint #5

Due to technological limitations, mirrors cannot currently be constructed for arbitrarily small values of γ_c for short cavity lengths. For example, the smallest value of γ_c is at least 10^6 s^{-1} for 1 cm cavities and at least 10^7 s^{-1} for 10 μm cavities. It then follows that a high enough frequency must be chosen so that constraint #4 can be satisfied using current technology.

4.6 Constraint #6

The reflectivity of the cavity R_c and the cavity decay rate are related by

$$R_c = 1 - \frac{2L\gamma_c}{c}. \tag{20}$$

The best mirrors have a reflectivity $R_c \approx 0.9999999$. Thus, it follows from equation (19)

$$1 - \frac{2L\gamma_c}{c} \leq 0.9999999,$$

or

$$\gamma_c \geq \frac{5 \times 10^{-8} c}{L}. \tag{21}$$

Equation (21) is an imposed constraint on the value of γ_c. The smallest cavity decay rate is inversely proportional to the length of the cavity.

Table 2. The parameters for a wavelength of 630 nm for frequencies of 300 Hz, 10 kHz, and 10 MHz. $\gamma_c \approx \overline{\gamma_D} \approx \omega_m$, $\eta = 0.8$, and $\Delta x = 10^{-14}$. For each frequency, $R = 0.9999999$ and $N \approx 4.45 \times 10^7$.

$\omega_m/2\pi$ (Hz)	γ_m (s^{-1})	P (W)	M (kg)	L (m)	g	T_E (K)
300	10^{-2}	3.50554×10^{-17}	5.59468×10^{-10}	1.12161×10^{-2}	9.00034×10^5	2.71391×10^{-3}
10^4	3×10^{-1}	1.16851×10^{-15}	1.6784×10^{-11}	3.36484×10^{-4}	1.00004×10^6	1.00515×10^{-1}
10^7	10^2	1.16852×10^{-12}	1.6784×10^{-14}	3.36484×10^{-7}	3.00012×10^6	3.01545×10^2

Table 3. The parameters for a wavelength of 800 nm for frequencies of 300 Hz, 10 kHz, and 10 MHz. $\gamma_c \approx \overline{\gamma_D} \approx \omega_m$, $\eta = 0.8$, and $\Delta x = 10^{-14}$ m. For each frequency, $R = 0.9999999$ and $N \approx 5.66 \times 10^7$.

$\omega_m/2\pi$ (Hz)	γ_m (s^{-1})	T_E (K)	M (kg)	L (m)	g	P (W)
300	10^{-2}	2.71391×10^{-3}	5.59468×10^{-10}	8.83271×10^{-3}	9.00034×10^5	2.76061×10^{-17}
10^4	3×10^{-1}	1.00515×10^{-1}	1.6784×10^{-11}	2.64981×10^{-4}	1.00004×10^6	9.20204×10^{-16}
10^7	10^2	3.01545×10^2	1.6784×10^{-14}	2.64981×10^{-7}	3.00012×10^6	9.20207×10^{-13}

Table 4. The algorithm used in the optimization.

Fixed Parameters: Δx, η
Input: λ, $\omega_m/2\pi$, κ, γ_m
1. $\gamma \rightarrow \omega_c$
2. $\omega_m/2\pi \rightarrow \omega_m$
3. Set $\gamma_c = \gamma_D = \omega_m$
4. Compute M using $\Delta x \sim \sqrt{\hbar/M\omega_m}$
5. Compute T_E using equation (10)
6. Check if $\Delta x > \lambda_{th}$
7. Compute N and L using equations (14) and (16)
9. Determine g by minimizing equation (12) with respect to ξ
10. Compute P using equation (13)

5 Numerical results

5.1 Optimization

A set of parameters is considered as optimal provided the following conditions are satisfied

a. the parameters must be experimentally feasible;
b. the parameters must satisfy the constraints;
c. the oscillating mirror must return to its ground-state energy within one period of its motion.

The optimization was performed first for a photon wavelength λ_c of 630 nm and then again for 800 nm. For each of these two wavelengths, three oscillator frequencies $\omega_m/2\pi$ were studied: 300 Hz, 10 kHz, and 10 MHz (see Tabs. 2 and 3).

Due to limitations imposed by current detection instrumentation, a value of 0.8 was chosen for η, the detection efficiency [1]. This guarantees a detection efficiency that is both relatively high and realizable with current technology. Also, to ensure maximum visibility for a given temperature, we set $\kappa = 1$. This ensures that the first constraint is satisfied. Finally, we fixed $\Delta x = 10^{-14}$ m. With the fixed parameter values set, the others can then be determined.

First, the relation $\Delta x \sim \sqrt{\hbar/M\omega_m}$ was used to determine the mass of the oscillating mirror. Next, the environmental temperature was computed from equation (10) using $\gamma_D = \omega_m$ satisfying contrainst #4. Equations (14) and (16) [with $\kappa = 1$] were then solved simultaneously to obtain the number of round-trips, N, the photon makes in the cavity and the length of the cavity L.

The gain factor g was determined by minimizing equation (12) with respect to ξ and finding the value of g that produced the ground-state (see Sect. 5.2). Finally, the intensity of the source light P was obtained using equation (13). The algorithm used to produce our results in outlined in Table 4.

5.2 Interference visibility and decoherence rate

5.2.1 Interference visibility

The interference visibility plotted as a function of $\omega_m t$ over one period of the mirror's motion at various temperatures for the three frequencies studied and a photon wavelength of 630 nm is shown in Figure 2. These figures illustrate that for a fixed frequency, interference visibility is strongly dependent on environmental temperature. As the temperature increases, decoherence sets in more rapidly. In fact, for increasingly higher temperatures, smaller fluctuations in temperature produce relatively larger effects on the visibility diagram.

However, the interference visibility's sensitivity to temperature is also dependent on frequency. As the mirror frequency is increased, relatively higher temperatures result in comparable visibility diagrams. Thus, we find the temperature requirements are relaxed as the frequency is increased. For example, as the frequency is increased from 10 kHz to 10 MHz, the optimized temperature increases from ∼101 mK to ∼302 K and yet the interference visibility diagrams are quite similar.

5.2.2 Decoherence rate

The decoherence rate is the rate at which decoherence of the photon and the oscillating mirror (photon-mirror system) occurs. Upon becoming incident to the mirror the photon will become entangled with the mirror. This

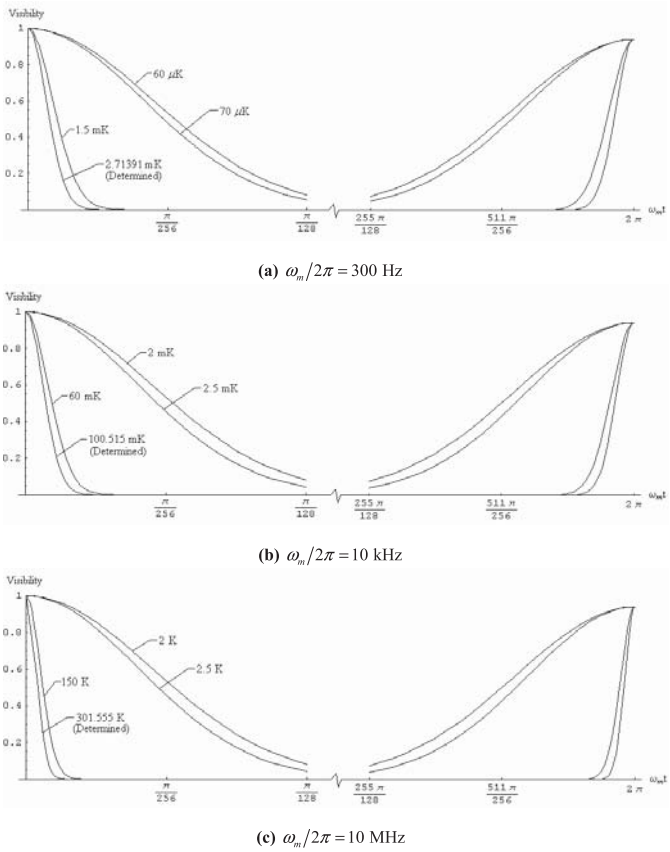

(a) $\omega_m/2\pi = 300$ Hz

(b) $\omega_m/2\pi = 10$ kHz

(c) $\omega_m/2\pi = 10$ MHz

Fig. 2. Interference visibility plotted as a function of $\omega_m t$ over one period of the mirror's motion for various oscillator frequencies ranging from 300 Hz to 10 MHz.

entanglement will continue for one full oscillation of the mirror's motion. If decoherence occurs too rapidly, then a valid measurement can not be made. Conversely, having some decoherence at the end of a period is desirable; since, the path differences of the photon due to decoherence will be measurable.

Environmental factors, particularly temperature, play a significant role in the decoherence rate. Figures 3a–3c show how the decoherence rate varies over one period of the mirror's motion for each of the three frequencies studied at several temperatures for a photon wavelength of 630 nm. It is clear from these figures that there is a strong correlation between decoherence rate and environmental temperature; decoherence rate increases with increasing temperature [14].

Figure 3d shows the logarithm of the decoherence curves for the three cases studied, plotted together in the same graph. Here, we see that decoherence rate is also dependent on frequency. As the frequency increases, the maximum decoherence rate increases. Moreover, as the temperature is reduced, the corresponding decoherence rate tends to near zero. This indicates that when the temperature is reduced, the corresponding decoherence rate will be relatively smaller, perhaps ∼1% (or possibly even less) of its value at the higher temperatures.

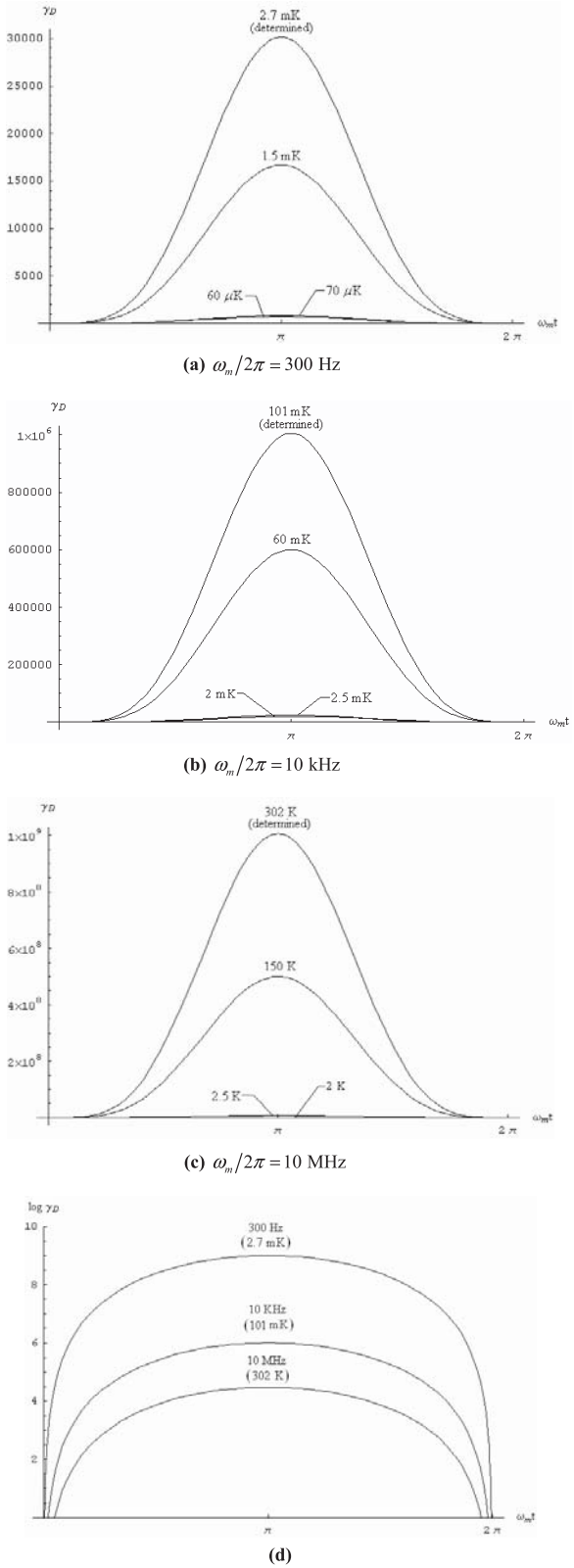

(a) $\omega_m/2\pi = 300$ Hz

(b) $\omega_m/2\pi = 10$ kHz

(c) $\omega_m/2\pi = 10$ MHz

(d)

Fig. 3. (a–c) Decoherence rate plotted as a function of $\omega_m t$ over one period of the mirror's motion for various oscillator frequencies ranging from 300 Hz to 10 MHz. (d) The logarithm of the decoherence rate as a function of $\omega_m t$ over one period of the mirror's motion with all three frequencies shown together (at the optimal temperatures).

5.3 Determination of the ground-state

Suppose the equation defining E_c is differentiated with respect to ξ. Then

$$\frac{dE_c}{d\xi} = -\frac{\left(g^2 - 2\eta\xi^2\right)\hbar\omega_m}{4\left(1+g\right)\eta\xi}. \tag{22}$$

Setting the derivative equal to zero and solving for ξ, gives

$$\xi = \frac{g}{\sqrt{2\eta}}. \tag{23}$$

Substituting equation (19) into equation (16) produces

$$E_c^{min} = \frac{k_B T_E}{1+g} + \frac{\hbar\omega_m g}{\sqrt{2\eta}\,(1+g)} \tag{24}$$

which is the minimum value of the energy as a function of the gain factor g. When there is no gain factor, i.e., when $g = 0$, the minimum energy is $E_c^{min} = k_B T_E$. Moreover, as the gain factor increases without bound, i.e., as $g \to \infty$, the minimum energy tends to the value $E_c^{min} = \hbar\omega_m/\sqrt{2\eta}$. Thus, for a given set of parameters, the minimum energy is bounded for all g.

In this experiment, we want the mirror to return to its ground-state within one cycle of its motion; that is, we want $E_c = \hbar\omega_m$. Substituting this value into equation (24) and solving for g gives

$$g = \frac{\sqrt{2\eta}\left(k_B T_E - \hbar\omega_m\right)}{\left(\sqrt{2\eta} - 1\right)\hbar\omega_m}. \tag{25}$$

When the gain factor is equal to this value, the mirror will return to its ground-state.

E_c^{min} (scaled by a factor of $2/\hbar\omega_m$) is plotted against g in Figure 4 for a photon wavelength of 630 nm. The plot shows the energy for each of the three oscillator frequencies we examined. Here we see that for a given cavity decay rate, E_c^{min} decreases monotonically with increasing g. Moreover, if the damping rate of the oscillator remains constant (as in the 300 Hz and 10 kHz cases), the value of g that produces a ground-state increases with increasing oscillator frequency.

5.4 Photon source intensity

Once g is determined, its value along with equation (23) can used to find the intensity of the photon source light P

$$P = \frac{M\gamma_m\omega_m\lambda L^2 g}{64\pi c\sqrt{2\eta}}\gamma_c^2. \tag{26}$$

The intensity of the source light is plotted against the square of the cavity decay rate in Figure 5 for each of the three frequencies studied. Here we see that for a fixed cavity decay rate, the required intensity increases with increasing mirror frequency [15].

It is worth noting that for a mirror frequency of 10 MHz, the intensity required for $\gamma_c \approx 10^7$ s^{-1} is very small ($\sim 10^{-12}$ W) [16]. On the other hand, for the mirror frequency of 500 Hz, the authors of [1] had an intensity of $\sim 10^{-8}$ W. Moreover, this intensity was achieved with the same cavity decay rate ($\gamma_c \approx 10^7$ s^{-1}). However, this decay rate is substantially higher than demanded by the constraints [2]. Our analysis reveals that a lower intensity is required while still using a realistic value for γ_c.

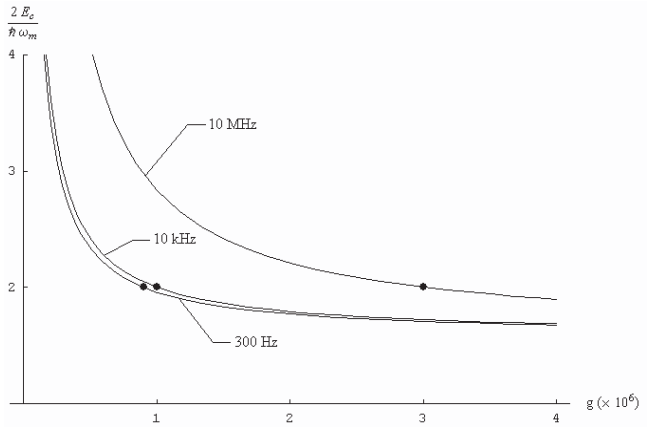

Fig. 4. A plot of the minimum energy of the cooled mirror vs. gain factor for various oscillator frequencies ranging from 300 Hz to 10 MHz. The points are the optimized values of g.

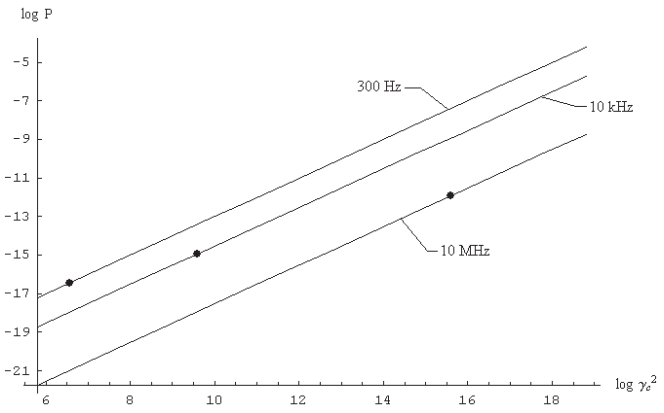

Fig. 5. A log-log plot of the photon source intensity as a function of the square of the cavity decay rate for various oscillator frequencies ranging from 300 Hz to 10 MHz.

Another concern when considering laser output is how much disturbance the laser will cause to the environment. If the laser intensity is too high, the laser can have the opposite effect on the mirror's environment than that intended. That is, a high laser intensity may actually increase environmental temperature [11]!

5.5 Reflectivity

In Figure 6a, the reflectivity is plotted as a function of cavity decoherence rate for each of the three frequencies investigated. As can be seen from the figure, the mirror

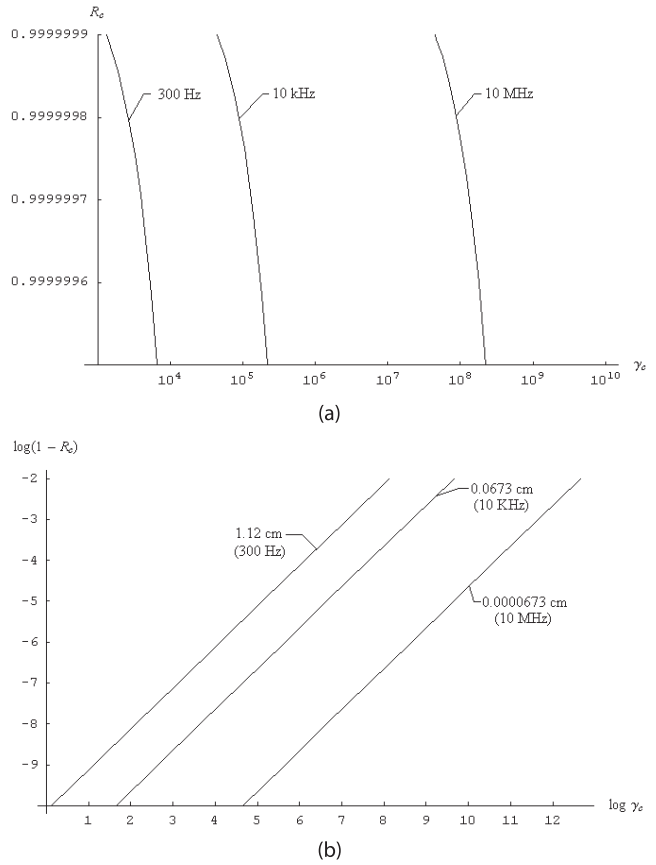

Fig. 6. A plot of (a) mirror reflectivity as a function of cavity decay rate for various oscillator frequencies ranging from 300 Hz to 10 MHz and (b) $\log(1-R_c)$ vs. $\log\gamma_c$ for the (optimized) cavity lengths corresponding to the same frequencies.

reflectivity requirements are independent of mirror frequency since the cavity decay rate is bound by the constraint $\gamma_c \lesssim \overline{\gamma_D} \lesssim \omega_m$; i.e., the reflectivity requirements remain constant as ω_m increases from 300 Hz to 10 MHz. Note that in our analysis, we had $\gamma_c = \overline{\gamma_D} = \omega_m$.

In Figure 6b, $\log(1 - R_c)$ is plotted against $\log \gamma_c$ for the three lengths determined through our analysis. This figure demonstrates two things. First, *without regard to constraints*, if γ_c remains fixed, then the mirror reflectivity requirements are relaxed as the length of the cavity is increased. As an example, for a mirror frequency of 10 MHz, $\gamma_c \approx 10^7$ s^{-1}, and mirror reflectivity requirements are relaxed from ∼0.9999999 to about ∼0.999 as the length of the cavity is increased from ∼0.000067 cm to ∼1.1 cm [3].

Second, if we assume each length corresponds to a specific frequency, then Figure 6b confirms the information conveyed by Figure 6a. As cavity length is increased, then for the constraint $\gamma_c \lesssim \overline{\gamma_D} \lesssim \omega_m$, the mirror reflectivity must remain fixed. In other words, as frequency is increased (hence as length is increased), the constraint $\gamma_c \lesssim \overline{\gamma_D} \lesssim \omega_m$ demands a fixed mirror reflectivity!

6 Discussion

Our investigations led to the determination of a mirror frequency of 10 MHz as optimal. At this frequency, not only was the ground-state achieved; but, it was achieved for a physically realizable cavity decay rate γ_c. This is important, since, current mirror technology sets restrictions on the minimum value of γ_c that can not be ignored. As a result of this restriction on γ_c, the values of many of the constraint quantities are restricted. The conclusions drawn from the 10 MHz case are summarized below.

First, temperature restrictions on interference visibility were greatly relaxed. In particular, our analysis revealed that as mirror frequency is increased, the relatively higher temperatures produce similar interference visibility. For example, the interference visibility obtained in the 10 MHz case for a temperature of ∼302 K was comparable to the value corresponding to the 300 Hz case for a temperature of ∼2.7 mK. For a given frequency, as temperature is increased the movable mirror system becomes decoherent. Moreover, coherence is destroyed within a fraction of the cycle.

Second, a strong temperature dependence of the decoherence rate was revealed. Decoherence rate increases with increasing temperature. Moreover, this increase becomes more pronounced for relatively higher temperatures. As with interference visibility, decoherence rate is also dependent on mirror frequency. As the frequency is increased, the maximum decoherence rate also increases. Again, the difference in maximum decoherence rate between two frequencies increases as the frequency is increased.

Third, for the 10 MHz case, ground-state energy was obtained for a significantly lighter mirror. This was due in part by keeping the separation Δx fixed at 10^{-14} m [in fact, Δx remained constant for all frequencies] and by the need for a much shorter optical cavity [∼0.3 μm]. This resulted in less spreading of the beam, thereby requiring a much smaller, lighter mirror [on the order of 10^{-14} kg]. Such cavities have been fabricated [4]. A smaller mirror has two advantages. Small, relatively lighter mirrors are easier to put into a superposition state as well as return to ground-state. Further, smaller mirrors can be coated uniformly more easily than larger mirrors. Thus, although the reflectivity demands remain the same regardless of frequency, these demands are easier to meet.

Fourth, a much lower source light intensity was needed to return the mirror to its initial energy state. A lower intensity results in less external interference. In fact, if the source light's intensity is too large, it may add heat to the system, bringing the temperature to undesirable levels. At the same time, the gain factor was not significantly altered from that given in [1]. In fact, the gain factor was quite similar in all three of frequencies we studied. As with the intensity of the source light, the gain factor should not become too large to minimize disturbance to the mirror's environment.

The optimized parameter regime (see Tabs. 2 and 3) determined through our investigations could prove useful in the field of Quantum Computing and this is a motivating factor in our work. In large quantum systems,

environmentally induced decoherence sets in over time inducing errors into the computations [6]. The system described in this paper, with the optimal parameter regime we developed, would provide the experimenter with the ability to put a bacterium sized object into a superposition of states and maintain coherence of the system on a time interval over which measurements could be recorded. These measurements when applied to quantum error correction, could be used as a gauge to monitor the level of decoherence in the quantum system, allowing adjustments to be made as needed thereby minimizing error.

References

1. W. Marshall, C. Simon, R. Penrose, D. Bouwmeester, Phys. Rev. Lett. **91**, 130401 (2003)
2. C.K. Law, Phys. Rev. A **51**, 2537 (1994)
3. C.J. Hood, H.J. Kimble, Jun Ye, Phys. Rev. A **64**, 033804 (2001)
4. S. Bose, K. Jacobs, P.L. Knight, Phys. Rev. A **59**, 3204 (1999)
5. R. Feynman, Int. J. Theor. Phys. **21**, 467 (1982)
6. I. Chuang, R. Laflamme, P. Shor, W. Zurek, Science **270**, 1633 (1995)
7. W. Unruh, Phys. Rev. A **51**, 992 (1995).
8. D.G. Cory et al., Phys. Rev. Lett. **81**, 2152 (1998)
9. I. Tittonen et al., Phys. Rev. A **59**, 1038 (1999)
10. J. Yang, T. Ono, M. Esashi, Appl. Phys. Lett. **77**, 3860 (2000)
11. S. Mancini, D. Vitali, P. Tombesi, Phys. Rev. Lett. **80**, 688 (1998)
12. S. Mancini, V.I. Man'ko, P. Tombesi, Phys. Rev. A **55**, 3042 (1997)
13. D. Vitali, S. Mancini, L. Ribichini, P. Tombesi, J. Opt. Soc. Am. B **20**, 1054 (2003)
14. A.D. Armour, M.P. Blencowe, K.C. Schwab, Phys. Rev. Lett. **88**, 148301 (2002)
15. J.I. Cirac, M. Lewenstein, K. Moîlmer, P. Zoller, Phys. Rev. A **57**, 1208 (1998)
16. H.J. Mamin, D. Rugar, Appl. Phys. Lett. **79**, 3358 (2001)
17. P.F. Cohadon, A. Heidmann, M. Pinard, Phys. Rev. Lett. **83**, 3174 (1999)